

## An adiabatic calorimeter for small samples The solid–liquid system naphthalene–durene

J.C. van Miltenburg<sup>\*</sup>, G.J.K. van den Berg, A.C.G. van Genderen

<sup>a</sup>Chemical Thermodynamics Group, Debye Institute, Utrecht University, Padualaan 8, 3584 CH Utrecht, The Netherlands

Received 22 May 2001; received in revised form 24 June 2001; accepted 27 July 2001

### Abstract

The construction and calibration of an adiabatic calorimeter for samples of about 0.4 g is described. The calorimeter works between 10 and 420 K, the accuracy is 0.5% for heat capacity measurements and 0.2% for latent energy effect like the enthalpy of fusion. The solid–liquid phase diagram of the system naphthalene–durene is presented. The phase diagram has been determined by three measurements, the interrupted way of measuring in adiabatic calorimetry was used to calculate the liquid composition at different enthalpy levels. The phase diagram is an example of an almost ideal eutectic system. The excess Gibbs energy of the liquid phase at 360 K was found to be in the order of  $100 \text{ J mol}^{-1}$  for the equimolar mixture. © 2002 Elsevier Science B.V. All rights reserved.

*Keywords:* Calorimetry; Adiabatic; Naphthalene; Durene; Phase diagram

### 1. Introduction

We describe in this article the construction of an adiabatic calorimeter for samples of about  $0.6 \text{ cm}^3$ . The sample volume used in adiabatic calorimetry has been diminished from about  $100 \text{ cm}^3$  in the beginning of the last century to  $1\text{--}10 \text{ cm}^3$  for recent designs. Using still smaller samples does lead to the difficulty that the difference in heat capacity of vessel and compound and the empty vessel (tare) does become a small fraction of that of the empty vessel. This increases the inaccuracy of the measurement. One way to reduce this effect is to remove the thermometer from the sample vessel and to place it on the inner adiabatic shield [1]. The thermocouple signal, which

measures the difference in temperature between this shield and the vessel, is then used to correct the temperature of the shield to that of the vessel. Reduction of the tare heat capacity in this way is attractive, but some precision in the temperature measurement is lost. Direct measurement of the temperature using a platinum or rhodium–iron sensor and an automatic ac-bridge leads to a precision of about  $10^{-4}$  K. When the temperature is measured on the inner shield, the possible error in the derived temperature of the vessel is estimated to be  $10^{-2}$  to  $10^{-3}$  K, depending on the temperature and the quality of the control system that regulates the temperature of the shield. In the calorimeter described, we opted for a construction using a holder equipped with heater and thermometer in which the sample vessel fits closely.

An advantage of using a small sample vessel ( $<1 \text{ cm}^3$ ) is its simple construction. In larger vessels, we use a neck with a stainless steel rim. On this rim, a

<sup>\*</sup> Corresponding author. Tel.: +31-30-2532386;  
fax: +31-30-2533946.  
E-mail address: miltenb@chem.uu.nl (J.C. van Miltenburg).

gold plate is pressed by a screw cap for vacuum closure. In the small vessel the same construction is used, but the rim has the same dimension as the vessel. This makes it very easy to load and remove the compounds, which would be impossible to measure in the larger vessels. For instance, we measured wood chips, cocoa beans and apiezon vacuum grease.

As an example of the use of this kind of calorimeter and to show that sometimes a phase diagram can be measured precisely with only a few measurements, the solid–liquid system naphthalene–durene was measured. This system is known to be eutectic, the phase diagram has been published by Bassi et al. [2], but the liquidus data and the derived excess properties of the liquid state did not seem to be completely reliable.

## 2. Construction of the calorimeter

The calorimeter (laboratory design indication cal-8) is a scaled down version of CAL-V, of which the construction was described in 1987 [3] and improvements in design and software in 1998 [4]. A schematic drawing is given in the Fig. 1a and b. The cryostat consists of a liquid nitrogen tank of 0.5 dm<sup>3</sup>, a liquid helium tank of 0.7 dm<sup>3</sup> and an economiser, which is cooled by the evaporating helium gas. For low temperature measurements, both tanks are pre-cooled with liquid nitrogen for at least 24 h; the liquid nitrogen is blown out of the lower container and it is filled with liquid helium. One such filling allows measurements between 4.2 and 80 K for about 24 h before the liquid helium evaporates. The calorimeter vessel and the adiabatic shields are mounted in the space below the liquid helium tank. This space is separated from the main vacuum system by an O-ring closure, using a teflon ring. It is evacuated using a by-pass tube and when quick cooling of the vessel is needed, this space can be filled with a small helium pressure. This construction avoids large losses of liquid helium during the cooling of the vessel. Cooling the vessel from room temperature to 80 K takes about 2 h, and from 80 to 5 K takes 30–50 min. More details of the construction of the cryostat are given in Fig. 1a.

The calorimeter vessel is constructed of bronze; a gold plate is pressed by a screw cap on the sharp edge of the vessel using a torque of about 8 N m. This way of vacuum closing the vessel has proved to be satisfactory.

The dimensions of the vessel and the vessel holder are given in Fig. 1b. The holder is equipped with a heater (150  $\Omega$ , bifilarly wound) and a 25  $\Omega$  Rh/Fe thermometer. Oxford Instruments calibrated the thermometer between 13 and 300 K to within 0.002 K. The melting points of naphthalene and indium were used to extend the calibration to 420 K. The thermometer scale being the ITS-90 scale [5]. Molar masses were calculated using the IUPAC tables of 1991 [6,7].

The measuring procedure and the regulation of the two adiabatic shields and the wire heater are similar to the earlier described procedures [3,4].

## 3. Calibration and checking of the calorimeter

Measurements were made on synthetic sapphire [6,7] and *n*-heptane. The data were compared to smoothed literature values [8,9] at every 10 K between 10 and 400 K. Below 30 K, deviations are within 1–3%, between 30 and 50 K 1% and above 50 K within 0.2%. The deviations in terms of percentage are shown in Fig. 2. The precision of the calorimeter was derived from repeated measurements of the enthalpy of fusion of *n*-heptane and from standard deviations of polynomial fits of the heat capacity. For the enthalpy of fusion of *n*-heptane (four experiments) we found  $(14028 \pm 15)$  J mol<sup>-1</sup>, the standard uncertainty corresponds to about 0.1%. The literature value [9] is  $(14022 \pm 9.4)$  J mol<sup>-1</sup>. Using third-order polynomial fits over overlapping temperature regions of about 50 K, showed deviations within a band of 0.2% above 80 K. Below 80 K, deviations up to 0.6% were found.

## 4. The naphthalene–durene system

The components, naphthalene and durene, were bought from Merck, the stated purity being >99%. Both compounds were first measured as received. All experiments were performed with stabilisation periods of 2000 s and heating periods of about 600 s. The actual melting procedure took about 4 h, measuring from 300 to 370 K took 24 h. This slow heating rate assured that thermal equilibrium was reached in the melt. Exponential extrapolation to infinite time of the temperature in the stabilisation periods in the melt differed by 0.001 K or less from the last measured temperatures.

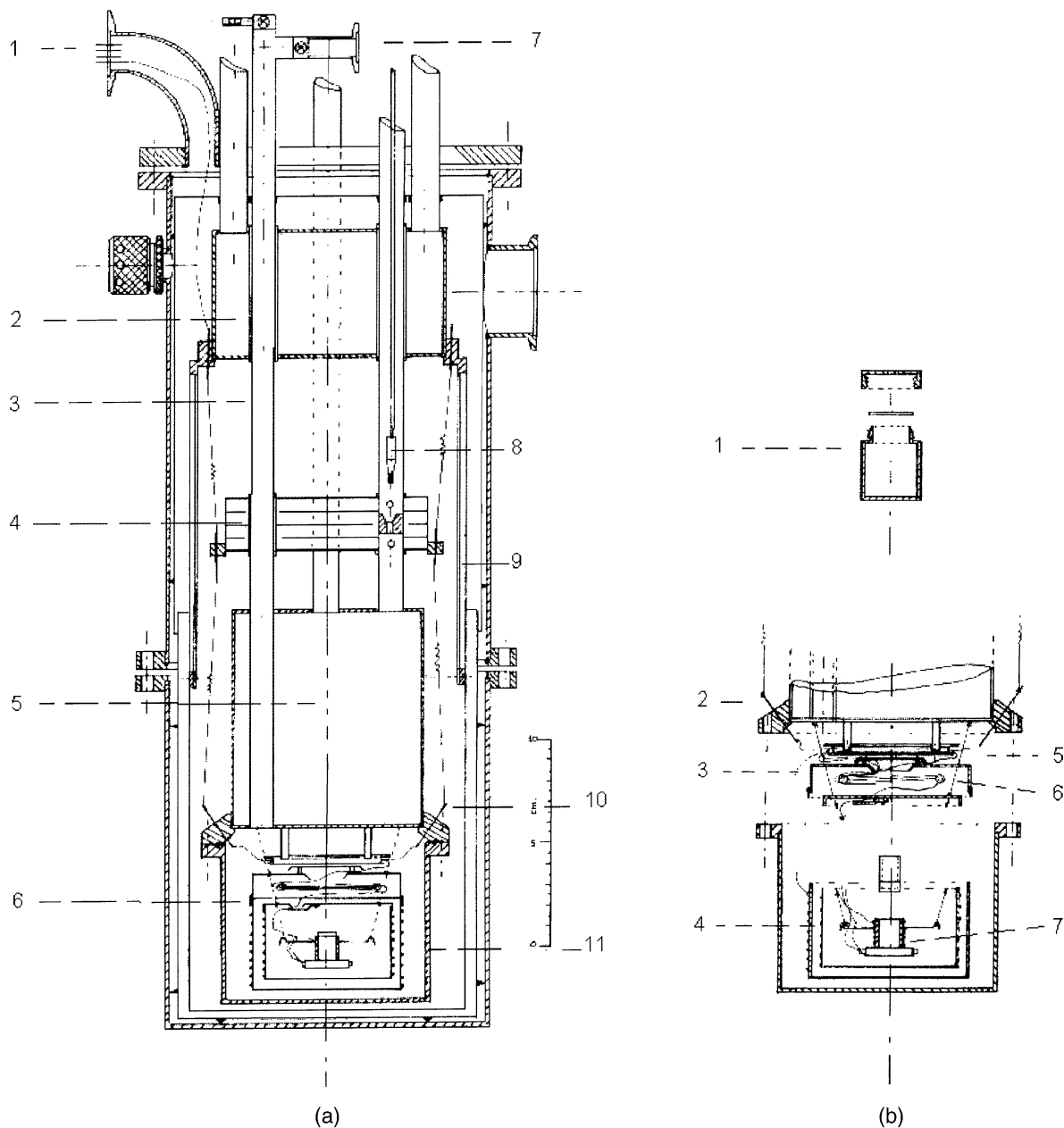


Fig. 1. (a) Schematic view of the cryostat and the calorimeter (1) wire feed-through; (2) liquid helium tank, 0.5 l; (3) one of the stainless steel tubes, diameter 10 mm, wall thickness 0.25 mm, the tube leading into the calorimeter space contains a radiation shield; (4) economiser, gas flow is forced through by lowering (8); (5) liquid helium tank, 0.7 l; (6) calorimeter space, see b; (7) vacuum by-pass and gas-inlet; (8) fibre glass stick; (9) double-walled gold-plated radiation shield; (10) wire feed-through to the calorimeter space, this feed through is constructed of a lacquered copper wire, which is drawn through a highly polished hole; (11) copper shield. (b) The calorimeter (1) vessel, closed with a gold plate, scale about 1:1; (2) bottom of the helium container; (3) lid of the outer adiabatic shield; (4) outer and inner adiabatic shields; (5) teflon disk used to wrap the incoming wires; (6) wire heater; (7) holder equipped with heater and thermometer.

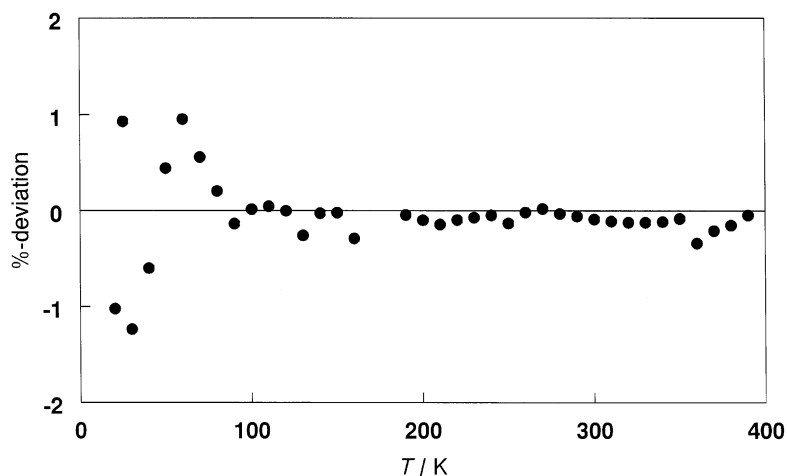


Fig. 2. Deviation plot of the experimental and literature values of the heat capacity of synthetic sapphire and *n*-heptane.

Plotting the reciprocal of the melted fraction against the equilibrium temperature resulted in straight lines, indicating that the impurities formed eutectic systems with the main components. As the compounds “as received” were not of very high purity, purification by vacuum sublimation and/or partial crystallisation was performed. For the partial crystallisation a metal block, equipped with heater and thermometer was used. A glass tube, containing the compound to be purified and a small magnetic stirrer, was inserted in the central hole. A metal cold finger, with small disks at the bottom, was inserted. After melting under a nitrogen flux, the cold finger was cooled with compressed air or water. See-through slits in the block allowed observing the crystal growth on and between the disks. When sufficient material was collected, the cold finger was raised above the liquid level, the glass tube replaced by a clean one and the crystallised material was collected. This procedure is quick; it takes about 1 h, while the vacuum sublimation procedure will take 1 or 2 days. Results of the different purification methods are given in Table 1. Both methods resulted for durene in a purity of 99.98%. As the starting material was of a purity of 99.31%, a significant improvement has been achieved.

For further calculations, the mean values for the enthalpy of fusion of the purified materials was used. These values are given by  $\Delta H_{\text{fus}}(\text{naphthalene}) = (19028 \pm 50) \text{ J mol}^{-1}$  and  $\Delta H_{\text{fus}}(\text{durene}) = (21623 \pm 80) \text{ J mol}^{-1}$ .

In the calculation of the phase diagram, the enthalpy of fusion of the pure components is considered to be a function of temperature. For the calculation the following fits for the solid (s) and liquid (l) state close to the normal melting point were used. The temperature region over which the fits were made is given.

For naphthalene

$$C_{p,s}(300 - 330) = -34.48 + 0.6771T$$

$$C_{p,l}(355 - 380) = 60.42 + 0.4455T$$

Table 1  
Melting temperatures, enthalpy of fusion and purity of naphthalene and durene samples

	$T_{\text{fus}}$ (K)	$\Delta H_{\text{fus}}$ (J mol <sup>-1</sup> )	Purity (mol%)
Naphthalene			
As received	353.22	19062	99.75
	353.28	19050	99.75
	353.32	19065	99.75
Partial crystallisation	353.40	19044	99.92
	353.40	19012	99.92
Durene			
As received	352.25	21448	99.31
	352.16	21384	99.39
Partial crystallisation	352.39	21650	99.98
Sublimation	352.36	21722	99.98
	352.39	21548	99.94
Sublimation followed by partial crystallisation	352.36	21722	99.98

For durenene

$$C_{p,s}(300 - 330) = 47.78 + 0.5746T$$

$$C_{p,l}(355 - 370) = 107.48 + 0.4584T$$

Three mixtures were measured; the mole fraction of naphthalene ( $x_{\text{naph}}$ ) being 0.0710, 0.5110 and 0.9324, respectively. The mass of the samples was between 0.4 and 0.5 g. The samples were first heated to about 10 K above the highest melting point and left at that temperature overnight. Controlled cooling at a rate of 3 K h<sup>-1</sup> was followed by a measurement under the same conditions at the pure components. All measurements were made twice. For each mixture, a table was constructed containing the equilibrium temperatures ( $T_{\text{eq}}$ ), the enthalpy increment without the contribution of the heat capacity of the solid and liquid ( $\Delta H$ ) and the enthalpy of fusion of the pure compounds as a function of temperature ( $\Delta H_{\text{naph}}$  and  $\Delta H_{\text{dur}}$ ). Assuming a eutectic system, the mole fraction of the liquid ( $x_1$ ) present at the different equilibrium temperatures was calculated by using (at the durenene rich side of the diagram)

$$x_1 = \frac{x_{\text{naph}}}{(\Delta H - x_{\text{naph}}\Delta H_{\text{naph}}(T_{\text{eut}}))/\Delta H_{\text{dur}}(T) + x_{\text{naph}}} \quad (1)$$

As an example, the calculation for the mixture with the overall composition  $x_{\text{naph}} = 0.071$  is given in

Table 2. The measured enthalpy curve is depicted in Fig. 3.

In Fig. 4, the equilibrium temperatures of the three mixtures and the melting points of the pure components are given. The data as published by Bassi et al. [2] are also depicted.

Assuming eutectic behaviour, the liquidus curves can be calculated using the relation [10]

$$-\int_{T_0}^T \Delta S_1^* + RT \ln(1-x) + \mu_1^E(l, T, x) = 0 \quad (2)$$

in which  $T_0$  is the melting point of the pure component 1,  $\Delta S_1^*$  the entropy of fusion of component 1 and  $\mu_1^E(l, T, x)$  the excess Gibbs energy of component 1 in the liquid phase. Using the regular solution model for the excess Gibbs energy and neglecting temperature influences, the excess Gibbs energy term in its most simple form becomes

$$\mu_1^E = Ax^2 \quad (3)$$

Combination leads to

$$T_{\text{liquidus}}(x) = \frac{\Delta H_1^* + Ax_1^2}{\Delta H_1^*/T_0 - R \ln(1-x_1)} \quad (4)$$

The hatched lines drawn in Fig. 4 represent the liquidus temperatures calculated with this relation. The solid lines were calculated assuming ideal behaviour ( $A = 0$ ). The hatched lines were calculated after optimising the value of  $A$  to 528 J mol<sup>-1</sup>.

Table 2

Calculation of liquid composition as a function of the equilibrium temperature for the mixture with overall composition  $x_{\text{naph}} = 0.071$

$T_{\text{eq}}$ (K)	$\Delta H$ (J mol <sup>-1</sup> )	Number of moles of durenene	$x_1$	$\Delta H(T)_{\text{dur}}$ (J mol <sup>-1</sup> )	$\Delta H(T)_{\text{naph}}$ (J mol <sup>-1</sup> )
323.337	2728	0.0672	0.5139	21029	18531
325.864	2941	0.0771	0.4795	21085	18581
328.354	3194	0.0888	0.4442	21139	18628
330.801	3507	0.1034	0.4071	21191	18674
333.195	3891	0.1212	0.3693	21242	18717
335.513	4371	0.1435	0.3310	21290	18757
337.727	4981	0.1718	0.2924	21336	18795
339.805	5760	0.2079	0.2546	21378	18829
341.713	6752	0.2539	0.2185	21416	18860
343.414	8001	0.3117	0.1855	21450	18886
344.877	9542	0.3830	0.1564	21479	18908
346.094	11386	0.4683	0.1316	21503	18926
347.078	13516	0.5669	0.1113	21522	18941
347.860	15889	0.6767	0.0950	21537	18952
348.478	18464	0.7958	0.0819	21549	18961
349.105	21037	0.9147	0.0710	21561	18970

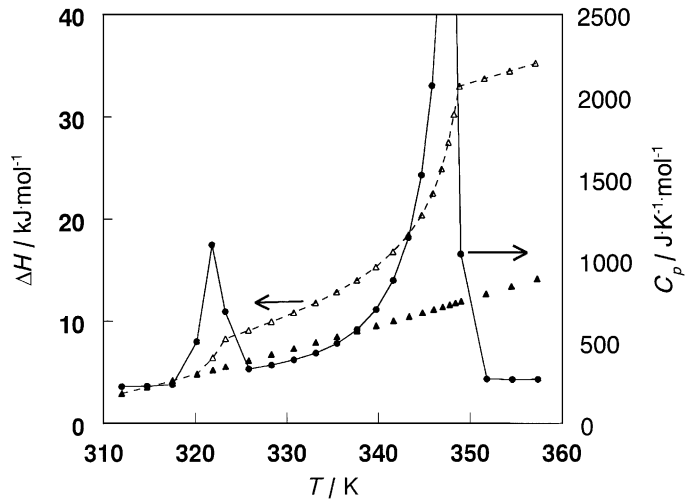


Fig. 3. Heat capacity and enthalpy measurement of the mixture  $x_{\text{naph}} = 0.071$  (●) heat capacity data; (△) enthalpy data; (▲) calculated base line.

From the specific heat measurement of the mixture with composition  $x_{\text{naph}} = 0.511$  the excess enthalpy and the excess entropy of the liquid could be calculated. Assuming a eutectic phase diagram, we found for the liquid phase the following excess properties.  $H_1^E = 218 \text{ J mol}^{-1}$  and  $S_1^E = 0.33 \text{ J K}^{-1} \text{ mol}^{-1}$  for the composition  $x_{\text{naph}} = 0.5$  at 360 K. The error margin is estimated to be about 25%, as the excess values are calculated as the differences of the large enthalpies of fusion. With these data and the measured heat capa-

cities of the liquid and the solid phase of the pure components, the phase diagram was calculated with the Winifit programme [11]. The excess enthalpy and the excess entropy of the liquid phase were assumed to be of the form

$$F_1^E = Cx(1-x) \quad (5)$$

Both calculation methods yield an almost perfect fit of the experimental data as can be seen in Fig. 4. This is to be expected as the non-ideality of the system is very

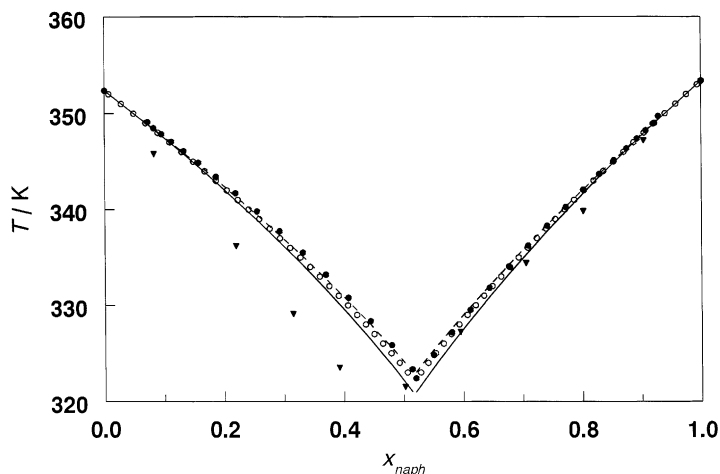


Fig. 4. The eutectic phase diagram of the durene–naphthalene system (●) experimental equilibrium points; (▼) data reference [2]; (○) Winifit calculation [11]; (—) calculation ideal diagram with  $A = 0$ ; (---) diagram with  $A = 528 \text{ J mol}^{-1}$ .

small, the regular model gives an excess Gibbs energy of the equimolar liquid at 360 K of  $132 \text{ J mol}^{-1}$ , the direct measurement of the excess properties leads to an excess Gibbs energy value of  $100 \text{ J mol}^{-1}$ . In view of the experimental uncertainty these values are comparable.

## 5. Discussion

The calorimeter described in this article is an instrument with which, in spite of the low sample mass used, reliable data can be obtained between 10 and 420 K. The accuracy and precision are less than the values obtained in our earlier constructed calorimeters, but the instrument is useful for small samples or samples which are difficult to load in the calorimeter vessel.

The binary system naphthalene–durene is a good example of an almost ideal eutectic system. The excess Gibbs energy calculated for the liquid phase is small.

## References

- [1] M. Grubert, Th. Ackermann, *Z. Phys. Chemie Neue Folge* 93 (1974) 255.
- [2] P.S. Bassi, R.P. Sharma, J.R. Khurma, *Indian J. Technol.* 29 (1991) 115.
- [3] J.C. van Miltenburg, G.J.K. van den Berg, M.J. van Bommel, *J. Chem. Thermodyn.* 19 (1987) 1129.
- [4] J.C. van Miltenburg, A.C.G. van Genderen, G.J.K. van den Berg, *Thermochim. Acta* 319 (1998) 151.
- [5] H. Preston-Thomas, *Metrologia* 27 (1990) 3.
- [6] Atomic Weights of the elements 1991, IUPAC, *Pure Appl. Chem.* 64 (1992) 1519.
- [7] N.B.S. standard reference material 720, Washington DC 1982.
- [8] D.A. Archer, *J. Phys. Chem. Ref. Data* 22 (1993) 1441.
- [9] T.B. Douglas, G.T. Furukawa, R.E. McCoskey, A.F. Ball, *J. Res. Natl. Bureau Standards* 53 (1954) 139.
- [10] H.A.J. Oonk, *Phase Theory, Studies in Modern Thermodynamics* 3, Elsevier, Amsterdam, 1981.
- [11] D. Daranas, R. López, D.O. López, WINIFIT 2.0: A Windows Computer Program for the Thermodynamic Assessment of T-X Phase Diagrams, Polytechnic University of Catalonia, Barcelona, 2000.